

INTERRELATIONSHIPS BETWEEN THE PHASE DIAGRAMS OF THE TWO-COMPONENT PHOSPHOLIPID BILAYERS

ISTVÁN P. SUGÁR*‡ AND GIANLUIGI MONTICELLI§

**Department of Biochemistry, University of Virginia, Charlottesville, Virginia 22908; ‡Institute of Biophysics, Semmelweis Medical University, 1444 Budapest, Hungary; and §Istituto di Fisiologia generale e Chimica Biologica, Università degli Studi, 20133 Milano, Italy*

ABSTRACT Basic relationships between the phase diagrams, previously considered independent of each other, are described. Phase diagrams of two-component phosphatidylcholine/phosphatidylcholine (PC/PC), phosphatidylethanolamine/phosphatidylethanolamine (PE/PE), and PC/PE lipid membranes are systematically investigated by means of the Landau theory. While gradually changing the chain length of one of the components, a characteristic peritectic-miscible-azeotropic-semiazeotropic-eutectic (P-M-A-S-E) series of the phase diagram was found in the PC/PE system and a peritectic-miscible-one-component-miscible-peritectic (P-M-O-M-P) series was found in the PC/PC and PE/PE systems. These serial catastrophic changes in the phase diagrams could be explained by the fusion and birth of the mixed phase regions in the phase diagram. Finally when we constructed the superdiagrams, we obtained all of the possible series of the phase diagrams in a wide class of the two-component mixtures. Moreover, one can predict the type of the phase diagram when the components r and p contain equal-length saturated hydrocarbon chains. Depending on the relationships between the chain lengths (L_r , L_p) and that on the phase transition temperatures of the pure components (T_r , T_p), the system is: miscible (M), if $0 < T_r(L) - T_p(L) < 5^\circ\text{C}$ and $L_r - L_p \geq 0$, azeotropic (A), if $0 < T_r(L) - T_p(L) < 5^\circ\text{C}$ and $L_r - L_p < 0$, peritectic (P), if $T_r(L) - T_p(L) > 40^\circ\text{C}$ and $L_r - L_p \geq 0$, eutectic (E), if $T_r(L) - T_p(L) > 40^\circ\text{C}$ and $L_r - L_p < 0$, while it is M or P if $5^\circ\text{C} < T_r(L) - T_p(L) < 40^\circ\text{C}$ and $L_r - L_p \geq 0$, and E, S, or A if $5^\circ\text{C} < T_r(L) - T_p(L) < 40^\circ\text{C}$ and $L_r - L_p < 0$.

INTRODUCTION

It is well known that the type of phase diagram exhibited by a binary mixture depends upon the nature of the components. The various types of phase diagrams have been known for many years (1). The relationships between the types of diagrams, however, are not clear because it is difficult to vary by small increments the physical properties of the two components of the mixture when simple substances, such as C, Fe, Cu, etc., are used. However, if the components are members of a homologous series, it is relatively easy to vary the physical properties by forming binary mixtures of the homologous components. This has been done in recent liquid-crystal and model membrane studies by using phospholipid pairs in which each member of the pair has a different acyl chain composition. Thus, Mabrey and Sturtevant (2) have demonstrated that a miscible system (M) consisting of two phosphatidylcholine (PC)¹ becomes peritectic (P) when the hydrocarbon chain-

length difference between the components exceeds a critical value. Moreover, binary mixtures of different homologues such as PC with phosphatidylethanolamines (PE) gives a series of different phase diagrams (3, 4, 5, 6). We review briefly the basic types of phase diagrams in Appendix A.

Here the Landau theory is used to examine the properties of binary mixtures as a function of the composition and the temperature homologous molecules of PC/PC, PE/PE, and PC/PE. An examination of the phase diagrams thus reveals the basic principles of the catastrophic conversion of one type of phase diagram with another.

MODEL

Experimental determination of a detailed phase diagram or simply the deduction of the type of diagram is difficult. Wilkinson and Nagle (7) have discussed the distinction between the M and P systems in relation to the DMPC/DSPC and DMPC/D20PC mixtures. The main problem is the extremely slow rate of equilibration in the gel phase.

On the basis of the Landau theory, a model was recently constructed (3, 8) from which we can derive different types of phase diagrams of any PC/PC or PC/PE mixtures. Aside from its simplicity, the main advantage of this model is that the diagrams are obtained from the same thermodynamic state function without the usual subsequent parameter fitting procedures (9). Moreover, by continuously changing the acyl chain length of one component, one can observe the transformation process from one type of the phase diagram to another. A brief description of the model is given in Appendix B.

¹*Abbreviations used in this paper:* M, miscible system; A, azeotropic system; S, semiazeotropic system; P, peritectic system, E, eutectic system; O, one-component system; A point, azeotropic point; PE, phosphatidylethanolamine; PC, phosphatidylcholines; D12PC:L- α dilauroylphosphatidylcholine (DLPC), D14PC:L- α dimiristoylphosphatidylcholine (DMPC), D16PC:L- α dipalmitoylphosphatidylcholine (DPPC), D18PC:L- α distearoylphosphatidylcholine (DSPC).

RESULTS

By using the model, we can determine the types of phase diagrams for each PC/PC, PE/PE, and PC/PE mixture using the two homologous series of saturated diacyl compounds. The results are shown in Table I. Mixtures appearing in the boxes have been experimentally examined previously. Their phase diagrams are in agreement with our model results (see references 3 and 8). Obviously, in mixing the elements of one homologous series (see the sections PC/PC and PE/PE mixtures of Table I) the resulting matrix of the phase diagrams have to be symmetric about the main diagonal. This symmetry generally does not hold for the other diagonal, the subdiagonal. On one side of the subdiagonal the mixtures of the shorter chain components are plotted, while on the other side the longer chain components are plotted. Because the chain length differences, together with the absolute chain lengths, determine the phase transition properties of the mixtures (see Eqs. B1 and B2), the matrix of the phase diagrams cannot be symmetric about the subdiagonal.

An interesting feature of the phase diagram matrices in Table I is that a gradual change in the chain length of one component results in the typical sequences of catastrophic changes in the phase diagrams. Thus, in PC/PC systems the complete sequence of the changes is P-M-O-M-P, whereas in PC/PE systems the sequence is P-M-A-E, except for the first three rows of the matrix in the PE/PC mixture section of Table I. What is the reason for these favored sequences? Can the exceptions be explained?

DISCUSSION

To understand the reason for the serial catastrophic changes in the phase diagrams we continuously changed the chain length of the PC component L_{PC} ($= L_p$) in the model, while keeping the chain length of the other component the same L_{PE} ($= L_r = 14$). Fig. 1 shows the typical stages in the process of catastrophic changes. Obviously, these changes occur when there are relative changes in the

position of the mixed phase regions in the phase diagrams. That is, a catastrophic change takes place when (a) the separated mixed phase regions fuse with each other or vice versa, or (b) a new mixed phase region appears or disappears.

Fusion and Separation of the Mixed Phase Regions

Almost every change in the type of phase diagram can be explained by the fusion and separation of the mixed phase regions. When the mixed gel phase region, MG, fuses with the mixed liquid crystalline-gel phase region, M1, of the M system, a miscible \rightarrow peritectic (M \rightarrow P) change takes place (see the upper diagrams in Fig. 1). Only this type of catastrophic change occurs in the PC/PC and PE/PE mixtures. In A systems, fusion of the MG region with the M1 region results in the azeotropic \rightarrow semiazeotropic (A \rightarrow S) change, while further fusion of MG with the M2 region produces a semiazeotropic \rightarrow eutectic (S \rightarrow E) change (see the lower three diagrams in Fig. 1).

The relative position of the MG region is very important in determining the type of phase diagram. The position of MG region is characterized by the temperature, T_i , at the top of the MG region

$$T_i = (\sigma \cdot |\Delta L| + \gamma) / 2R, \quad (1)$$

where σ and γ are model parameters and $|\Delta L|$ is the absolute acyl chain-length difference of the components. This equation is derived in Appendix C. Comparing this equation with the state function for the mixtures given by Eq. B1, it is apparent that RT_i is proportional to the excess free-energy term and, consequently, is a measure of the nonideality of the mixture. According to the statistical mechanical interpretation of these parameters:

$$\sigma |\Delta L| \sim |U_{pp}^c - U_{rr}^c| \text{ and } \gamma \sim |U_{pp}^h - U_{rr}^h|,$$

where U_{ii}^c and U_{ii}^h are the nearest neighbor interaction energies in the gel phase between the acyl chains and the

TABLE I
PHASE DIAGRAM MATRICES OF THE TWO-COMPONENT PHOSPHOLIPID MEMBRANES

| L_r | Components from the same homologue series | | | | | | | | Components from different homologue series | | | | | | | | | | | | | | | |
|-------|---|----|----|----|----------------|----|----|-------|--|----|----|----|----|----|----|------------------|----|----|----|----|----|----|----|---|
| | PC/PC mixtures | | | | PE/PE mixtures | | | | PE/PC mixtures | | | | | | | | | | | | | | | |
| | 12 | 13 | 14 | 15 | 16 | 17 | 18 | L_r | 12 | 13 | 14 | 15 | 16 | 17 | 18 | $(L_{PE} =) L_r$ | 12 | 13 | 14 | 15 | 16 | 17 | 18 | |
| 12 | O | M | M | M | M | P | P | 12 | O | M | M | M | M | P | P | 12 | M | E | E | E | E | E | E | E |
| 13 | M | O | M | M | M | M | P | 13 | M | O | M | M | M | M | M | 13 | P | M | E | E | E | E | E | E |
| 14 | M | M | O | M | M | M | M | 14 | M | M | O | M | M | M | M | 14 | P | P | M | S | E | E | E | E |
| 15 | M | M | M | O | M | M | M | 15 | M | M | M | O | M | M | M | 15 | P | P | P | M | A | E | E | E |
| 16 | M | M | M | M | O | M | M | 16 | M | M | M | M | O | M | M | 16 | P | P | P | P | M | A | E | E |
| 17 | P | M | M | M | M | O | M | 17 | P | M | M | M | M | O | M | 17 | P | P | P | P | M | M | A | A |
| 18 | P | P | M | M | M | M | O | 18 | P | M | M | M | M | M | O | 18 | P | P | P | P | P | M | M | M |

The boxed-in phase diagrams were also experimentally determined (see references 2, 4, 5, 6, 7, 9).

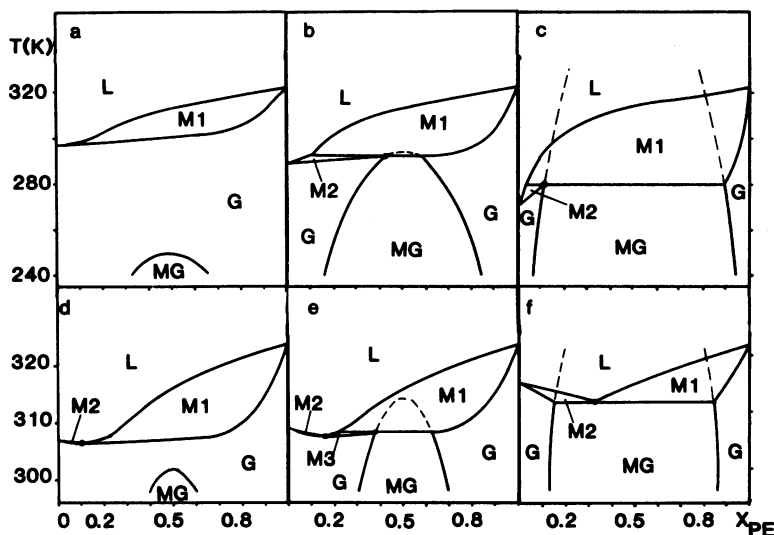


FIGURE 1 Typical stages in the transition processes of the phase diagrams when the chain length of PC component L_{PC} and consequently $L_{PC} - L_{PE} (= \Delta L)$ changes continuously in the model while the reference PE component remains constant, $L_{PE} = 14$ (DMPE). (a) $\Delta L = 0$, an M system; (b) $\Delta L = -0.7$, a P system; (c) $\Delta L = -2$, a P system; (d) $\Delta L = 0.8$, an A system; (e) $\Delta L = 1$, a S system; (f) $\Delta L = 2$, an E system. Solid lines, calculated phase diagrams. Dashed lines, metastable phase lines of the mixed gel, MG region. MG, M1, M2, M3: different mixed phase regions. X_{PE} , mole fraction of the reference PE component in the mixture. $T(^{\circ}\text{K})$: absolute temperature.

polar heads of the same components, respectively (3). γ therefore vanishes when each component has the same head group. The possible types of phase diagrams can be predicted using Eq. 1. Let T_s be the temperature of the solidus curve at $X_r = 0.5$. If $T_i < T_s$, the mixed phase regions are separated and the system is M or A, while it is P, E, or S if $T_i > T_s$. Usually T_s can be approximated simply by the smaller phase transition temperature of the

pure components: $T_s \approx \min \{T_r, T_p\}$. As an example in DMPE/DPPC system, $T_s \approx T_{DPPC} = 314.5^{\circ}\text{K}$ and $T_i = 375^{\circ}\text{K}$ at $\sigma/R = 125^{\circ}\text{K}$, $\gamma/R = 500^{\circ}\text{K}$ (see Appendix B) and $|\Delta L| = 2$. Consequently, the system is P, S, or E. We know from the experiments or from the PC/PE mixtures section of Table I that this system is E.

In Fig. 2 a, b the fusion lines show the critical values of L_p (where $T_s = T_i$) as a function of the reference chain

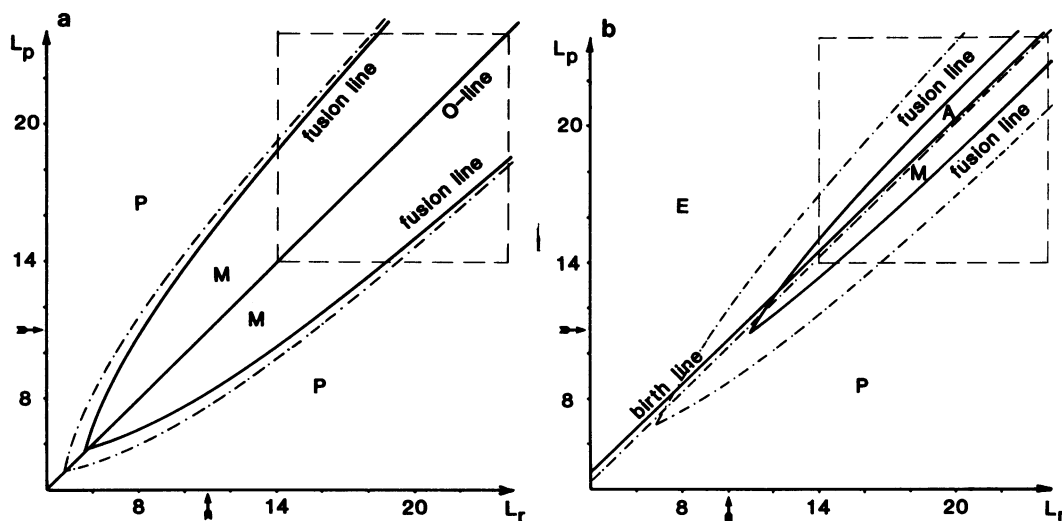


FIGURE 2 Superdiagrams of two-component phospholipid membranes. (a) Components from the same homologue series. Solid lines, PC/PC mixtures. Dot-dash lines, PE/PE mixtures. (b) Components from different homologue series. Solid lines, PC/PE mixtures. Dot-dash lines, mixtures of PC homologues with the elements of a hypothetical homologue series, characterized by $\gamma/R = 250^{\circ}\text{K}$, $L^* = 5.9$, $Z/R = -231.6^{\circ}\text{K}$, $W/R = -1,100.8^{\circ}\text{K}$. M, A, P, O, E represent the zones of the miscible, azeotropic, peritectic, one-component, and eutectic systems, respectively. The dashed lines frame the zone of the biologically important chain lengths (10). L_p and L_r are the chain lengths of the p and r components, respectively. In PC/PE mixtures $L_p = L_{PC}$ and $L_r = L_{PE}$. Arrows at $L_{PE} = 10$ and $L_{PC} = 11$ mark the validity limit of the model and the superdiagrams. The analytical continuations of the fusion and birth lines are also calculated outside the range of validity.

length, L_r . These kinds of fusion lines exist always when the pure components show single phase transitions and the phase transition temperatures are monotonically increasing functions of the acyl chain length. We note here that the validity limits of the applied model are at $L_{PE} = 10$ and $L_{PC} = 11$, where the respective phase transition enthalpies of the pure components are zero (3, 8). In spite of these limitations, the analytical continuations of the fusion lines are shown for $L_{PE} < 10$ and $L_{PC} < 11$ in Fig. 2 *a, b*.

Birth and Death of a Mixed Phase Region

The two branches of the catastrophic changes generated by fusions: $M \rightarrow P$ and $A \rightarrow S \rightarrow E$ can be connected by means of the $M \rightarrow A$ change. This change from M to A is the consequence of the birth of a new mixed phase region (see Fig. 1 *a, d*). Let us follow the details of this birth process in the case of PC/PE mixtures. At $\Delta L (= L_{PC} - L_{PE}) = 0$, the PC/PE mixtures create M systems. Here the MG and $M1$ regions are well separated (see Fig. 1 *a*). When ΔL is increased nonideality starts to increase, i.e., the MG region moves upwards and the $M1$ region starts broadening (Figs. 1 *a, d*). As ΔL increases, the transition temperature difference of the pure components, $T_{PE} - T_{PC}$, decreases. This and the broadening of $M1$ region causes the beginning slope of the solidus curve at $X_{PE} = X_r = 0$ to become zero (see Fig. 1 *d*). At this critical value of ΔL , a new mixed phase region is born and the phase diagram changes from M to A or from P to S depending upon whether MG is separated or fused, respectively. The new mixed phase, $M2$, and the old, $M1$, are separated by the A point (azeotropic point). Further increasing ΔL causes this point to move towards larger mole fractions and thus the proportion of $M2$ increases (see Figs. 1 *d, e*). Finally, at $\Delta L \approx 10$, the A point disappears at $X_{PE} = 1$ resulting in an $E \rightarrow P$ change. However, at this large value of ΔL , presumably the bilayer structure of the mixture itself is unstable and two different structures may coexist in the membrane: noninterdigitated bilayer for the shorter chain molecules and interdigitated bilayer for the longer chain molecules.

We note here that the birth of a new phase is necessary when the slope of the solidus curve becomes zero, otherwise a further increase in ΔL would cause the same solidus curve to contain a minimum near $X_{PE} = 0$. This would create an impossible mixed phase region containing gel-gel clusters below T_{PC} and gel-liquid crystalline clusters above it.

Solving a system of implicit equations (see Eqs. D3 and D4 in Appendix D) the critical values $L_{PC} (= L_p)$, where the A point appears, can be determined at different reference chain lengths $L_{PE} (= L_r)$. In Fig. 2 *b* the critical L_{PC} values, where the fusion and birth of the mixed phases take place, are plotted as a function of L_r . The (L_p, L_r) plane of this diagram is divided into four zones by fusion and birth lines (see solid lines in Fig. 2 *b*). Every zone

corresponds to one type of phase diagram. The region of the S systems (not shown in Fig. 2 *b*) is a very thin zone along the border line of the E zone. While different phases belong to the different regions of the phase diagrams, in the zones of these more abstract diagrams there are different kinds of phase diagrams. For this reason these diagrams are referred to as superdiagrams.

The experimentally realizable mixtures are situated in the integer points of the (L_p, L_r) plane. Obviously the phase diagram matrices in Table I or the possible sequences of the phase diagrams can be determined by means of these superdiagrams. According to this, the previously noted P-M-A-E sequence of the PC/PE phase diagrams exists if $L_{PE} \geq 15$, otherwise different sequences are obtained because the zones of A and M systems become narrow and disappear.

General Properties of the Superdiagrams

In the previous sections, special well-defined systems were treated. We can, however, generalize our results. In all cases where the components have saturated hydrocarbon chains of equal length, we can use the same form of the state function (Eq. B1) with different values for the model parameters and obtain qualitatively similar superdiagrams. Let us consider, for example, a mixture in which one of the components is PC. Let the interaction between the polar heads of the other hypothetical component be weaker than that of the PE polar heads and stronger than that of the PC polar heads. Thus, in these mixtures the polar heads of the components are more similar energetically than in the PC/PE system. Because of this similarity, the respective phase transition temperatures of the pure components $T_p(L)$ and $T_r(L)$ are closer to each other. In Fig. 2 *b* the dashed lines show the superdiagram of this hypothetical system. The model parameters of the hypothetical component were chosen to be the averages of the PC, PE model parameters ($\gamma/R = 250^\circ\text{K}$, $L^* = 5.9$, $Z/R = -231.6^\circ\text{K}$, $W/R = -1,100.8^\circ\text{K}$). Apparently, if the polar heads become energetically more similar, the M and A zones of the superdiagram become broader and the birth line moves closer to the 45° diagonal from the abscissa. At the same time in the zone of biologically important chain lengths (see the framed part in Fig. 2 *b*) the proportions of the M and A systems increase while that of the P and E systems decrease. Because the difference in the interaction energies between the polar heads can be characterized by $T_r(L) - T_p(L)$, we can use a more exact rule to predict the type of the phase diagram. That is, when the components contain equal-length saturated chains, the system is: M , if $0 < T_r(L) - T_p(L) < 5^\circ\text{C}$ and $L_r - L_p \geq 0$; A , if $0 < T_r(L) - T_p(L) < 5^\circ\text{C}$ and $L_r - L_p < 0$; P , if $T_r(L) - T_p(L) > 40^\circ\text{C}$ and $L_r - L_p \geq 0$; E , if $T_r(L) - T_p(L) > 40^\circ\text{C}$ and $L_r - L_p < 0$; while it is M or P if $5^\circ\text{C} < T_r(L) - T_p(L) < 40^\circ\text{C}$ and $L_r - L_p \geq 0$, and E, S , or A if $5^\circ\text{C} < T_r(L) - T_p(L) < 40^\circ\text{C}$ and $L_r - L_p < 0$.

The two types of the superdiagrams obtained (see Figs. 2 *a, b*) are fundamentally general. The following statements are valid for bilayer membranes and for any other system in which the organization of the molecules in the pure-component systems correspond to the organization in the respective mixed systems.

These kinds of fusion lines in Fig. 2 always exist if the pure-component systems show single phase transitions and T_r and T_p are monotonically increasing functions of the number of homologue units, L . The birth line always appears to cross the fusion line when the components of the mixtures belong to different homologue series. The chemical or qualitative difference between the components is reflected in the asymmetry of the superdiagram (see Fig. 2 *b*). The line system of the superdiagram will be almost symmetric about the 45° diagonal from the abscissa if the parameters, characterizing the two homologue series, are very close together, however, the arrangement of the zones still remains asymmetric (see the solid and dashed lines in Fig. 2 *b*). When the parameters become equal, i.e., the homologues become equivalent chemically, the superdiagram will be completely symmetric. The A, E, and S zones disappear and at the place of the birth line the O line will appear as the symmetry axis of the superdiagram. This dramatic change takes place because a qualitative difference, like a chemical difference, cannot vanish gradually.

In the symmetric superdiagrams, A, E, and S zones never appear. The A system and its consequences, the S and E systems, appear if the solidus line is horizontal at $X = 0$ or at $X = 1$, and $|T_r - T_p|$ decreases with increasing $|L_r - L_p|$. At the O line, the phase diagrams are horizontal lines and $|\Delta L| = 0, |\Delta T| = 0$. Consequently, close to the O line $|\Delta T|$ cannot decrease with increasing $|\Delta L|$. In addition, an A zone cannot appear far from the O line, since the symmetric superdiagram does not contain a birth line where the $M \rightarrow A$ change would take place.

Consequently, the sequences of the phase diagrams belonging to these two basic types of superdiagrams are also general. Namely, binary mixtures of different homologues result in P-S-E, P-M-P-S-E, or P-M-A-S-E sequences depending on the reference component, while mixtures belonging to the same homologue series produce P-M-O-M-P or P-O-P sequences.

APPENDIX A

Some Important Types of Phase Diagrams of Two-Component Mixtures

M System. This simplest phase diagram contains two separated mixed phase regions (see Fig. 1 *a*). In the M1 region, clusters coexist in the gel phase and in the liquid crystalline phase. At a given temperature T , the solidus line of M1 shows the mixing composition of the gel clusters, X_g , and the liquidus line shows the liquid crystalline clusters, X_c . In the MG region p-component-rich gel clusters and r-component-rich gel clusters coexist. In contrast with these mixed phase regions, the components are distributed homogeneously both in the liquid crystalline, L, and in the gel phase, G, regions.

A System. Except for the separated MG region, this diagram contains two connected mixed phase regions, M1 and M2 (see Fig. 1 *d*). The common point of four different phases is the A point (azeotropic point). In M1 region p-component-rich liquid crystalline clusters and r-component-rich gel clusters coexist, while in M2 the opposite is true.

P System. Three mixed phase regions (M1, M2, and MG) are connected with each other (see Fig. 1 *b, c*). M2 and MG are below a horizontal three-phase line and they are connected at a four-phase point, called the P point (peritectic point).

E System. Three mixed phase regions (M1, M2, and MG) are connected again but now M1 and M2 are above the horizontal three-phase line (see Fig. 1 *f*). M1 and M2 are connected at the E point (eutectic point), which is four-phase point.

S System. Four mixed phase regions (M1, M2, M3, and MG) are connected (see Fig. 1 *e*). Three of them (M1, M3, and MG) form a quasi-P system with a quasi-P point between M3 and MG. M2 and M3 are connected in a quasi-A point.

APPENDIX B

The state function of two-component PC/PC, PE/PE, and PC/PE membranes in RT units (R is the universal gas constant and T is the absolute temperature) is

$$G(X_r, S)/RT = X_r F_r(S)/RT + (1 - X_r) F_p(S)/RT + X_r \ln X_r + (1 - X_r) \ln(1 - X_r) + \Delta U \cdot X_r + 2(\sigma \cdot |\Delta L| + \gamma)(0.5 - S)X_r(1 - X_r)/RT, \quad (B1)$$

where X_r is the mole fraction of r (the reference) component; S is the disorder parameter, the fraction of C—C bonds in the hydrocarbon chains that is in the *gauche* conformation. L_p and L_r are the numbers of the C atoms in each acyl chain of the respective components. $\Delta L = L_p - L_r$ is the chain-length difference.

The first two terms in Eq. B1 are the linear combination of the free-energy functions of the pure components (one-component membranes of p and r). The next two terms denote the mixing entropy. The fifth term depends on the difference in the chemical potentials (ΔU) of the components. The last term, the excess free-energy term, is a measure of the nonideality of the mixture.

The free-energy function for a one-component bilayer $F(S)$ in RT units is

$$F(S)/RT = 2E_0(L - 3)S/RT + 2(L - L^*) [W(S - 0.39)^2 - Z(S - 0.39)^3 - W(0.39)^2 - Z(0.39)^3]/RT - (L - 2) 4 \sqrt{2} (S - S^2) \quad \text{at } S \geq 0 \text{ and} \\ F(S)/RT = \infty \quad \text{at } S < 0. \quad (B2)$$

Here the first term is associated with the intramolecular energy, the second term is the intermolecular energy term, and the third describes the configurational entropy of the hydrocarbon chains. The following model parameters are used: the *trans-gauche* energy difference $E_0 = 500$ cal/mol, $\sigma/R = 125^\circ\text{K}$, $\gamma/R = 500^\circ\text{K}$ for PC/PE mixtures, and zero for PC/PC and PE/PE systems; for PC homologues: $W/R = -1,085^\circ\text{K}$, $Z/R = -275^\circ\text{K}$, $L^* = 6.4$; for PE homologues: $W/R = -1,117.8^\circ\text{K}$, $Z/R = -188.3^\circ\text{K}$, $L^* = 5.4$. The physical meaning and the determination of these parameters can be found in references 3 and 8.

The state function $G(X, S)$ is used to determine the phase diagrams by determining the value or values of ΔU where two or three minima of the state function become global ones at a given temperature T . The compositions belonging to these minima determine the points of the phase lines of the diagram at T .

APPENDIX C

Position of the Mixed Gel Region

At a given T the values of the compositions X_{g1} and X_{g2} in the gel clusters of the MG phase are determined by the minima of the state function $G(X, S)$ at $S = 0$. Consequently, $G(X, 0)$ has one maximum and two inflection points within the (X_{g1}, X_{g2}) interval. The places of the inflection points are the solutions of the following second-order polynomial

$$\partial^2 G(X, 0)/\partial X^2 = -2(\sigma|\Delta L| + \gamma) + RT/[X(1 - X)] = 0. \quad (C1)$$

The solutions are symmetric with respect to $X = 1/2$

$$X_{1,2} = 0.5[1 \pm \sqrt{1 - 2RT/(\sigma|\Delta L| + \gamma)}]. \quad (C2)$$

The inflection points coincide at the top of the MG phase at $T = T_i$. In this case the discriminant becomes zero in Eq. C2, thus

$$T_i = (\sigma \cdot |\Delta L| + \gamma)/2R. \quad (C3)$$

APPENDIX D

Birth of the A Point

The characteristic feature of the A point is that the two global minima of $G(X_r, S)$ are at the same $X_r (= X_A)$ composition. Therefore, at the A point, the following equations exist:

$$\left. \frac{\partial G}{\partial X_r} \right|_{\substack{X_r = X_A \\ S = 0}} = \left. \frac{\partial G}{\partial X_r} \right|_{\substack{X_r = X_A \\ S = S_A}} = \left. \frac{\partial G}{\partial S} \right|_{\substack{X_r = X_A \\ S = S_A}} = 0 \quad (D1)$$

are the minimum conditions and

$$G(X_A, 0) = G(X_A, S_A) \quad (D2)$$

is the equilibrium condition. The values of the disorder parameter at the minima are zero and S_A .

Now, at a given reference chain length, L_r , what is the value of L_p where the A point appears? If $T_i(L) > T_p(L)$, then the A point appears at $X_r = 0 (= X_A)$ and at $T = T_p (= T_A)$ (see Fig. 1 d). With these two additional conditions, Eqs. D1 and D2 reduce into the system of two nonlinear equations:

$$[3B_p^2(A_r - A_p)/(16A_p^2) - 3B_p(B_r - B_p)/(8A_p) + C_r - C_p] \times R(\sigma|L_p - L_r| + \gamma)^{-1} = T_p^{-1} \quad (D3)$$

$$3B_p^2/(16A_p) = C_p, \quad (D4)$$

where A_i, B_i, C_i are the coefficients of the third-order polynomial of the free-energy function of i th component:

$$F_i(S; L_i, T_p)/[2RT_p] = A_i S^3/3 - B_i S^2/2 + C_i. \quad (D5)$$

Comparing Eq. B2 with Eq. D5 one can obtain coefficients that are functions of T_p and L_i . At a given L_r by means of Eq. D3 and Eq. D4, one can determine the unknown values of T_p and L_p where the A point appears.

We wish to thank Dr. C. Marzagora for computing assistance, Professors T. E. Thompson and R. L. Biltonen, Dr. P. L.-G. Chong, and W. van Osdol for critical evaluation of the manuscript before its submission. This research was supported by National Institutes of Health grant GM 14628, National Science Foundation grant PCM83-00056, and by an Italian Consiglio Nazionale delle Ricerche Public Health Project.

Received for publication 15 January 1985.

REFERENCES

- Landau, L. D., and E. M. Lifshitz. 1982. Statistical physics. In Course of Theoretical Physics. Part 1. Wheaton, A., and Co. Ltd., Exeter, England. 5:289-300.
- Mabrey, S., and J. M. Sturtevant. 1976. Investigation of phase transitions of lipids and lipid mixtures by high sensitivity differential scanning calorimeter. *Proc. Natl. Acad. Sci. USA.* 73:3862-3866.
- Sugár, I. P., and G. Monticelli. 1983. Landau theory of two-component phospholipid bilayers. I. Phosphatidylcholine/phosphatidylethanolamine mixtures. *Biophys. Chem.* 18:281-289.
- Blume, A., and T. Ackerman. 1974. A calorimetric study of the lipid phase transitions in aqueous dispersions of phosphorylcholine-phosphorylethanolamine mixtures. *FEBS (Fed. Eur. Biochem. Soc.) Lett.* 43:71-74.
- Chapman, D., and J. Urbina. 1974. Biomembrane phase transitions. Studies of lipid-water systems using differential scanning calorimeter. *J. Biol. Chem.* 249:2512-2521.
- Van Dijck, P. W. M., A. J. Kaper, M. A. J. Oonk, and J. deGier. 1977. Miscibility properties of binary phosphatidylcholine mixtures. A calorimetric study. *Biochim. Biophys. Acta.* 470:58-69.
- Wilkinson, D. A., and J. F. Nagle. 1979. Dilatometric study of binary mixtures of phosphatidylcholines. *Biochemistry.* 18:4244-4249.
- Priest, R. 1980. Landau phenomenological theory of one and two component phospholipid bilayers. *Mol. Cryst. Liq. Cryst.* 60:167-184.
- Lee, A. G. 1977. Lipid phase transitions and phase diagrams. II. Mixtures involving lipids. *Biochim. Biophys. Acta.* 472:285-344.
- Patton, G. M., J. M. Fasulo, and S. J. Robins. 1982. Separation of phospholipids and individual molecular species of phospholipids by high-performance liquid chromatography. *J. Lipid Res.* 23:190-196.